Journal of Virology

Frog Virus 3 Open Reading Frame 97R Localizes to the Endoplasmic Reticulum and Induces Nuclear Invaginations

Brooke A. Ring, Andressa Ferreira Lacerda, Dylan J. Drummond, Christina Wangen, Heather E. Eaton and Craig R. Brunetti

***J. Virol.* 2013, 87(16):9199. DOI: 10.1128/JVI.00637-13.**
Published Ahead of Print 12 June 2013.

Updated information and services can be found at:
http://jvi.asm.org/content/87/16/9199

These include:

REFERENCES

This article cites 36 articles, 13 of which can be accessed free at: http://jvi.asm.org/content/87/16/9199#ref-list-1

CONTENT ALERTS

Receive: RSS Feeds, eTOCs, free email alerts (when new articles cite this article), more»

Information about commercial reprint orders: **http://journals.asm.org/site/misc/reprints.xhtml**
To subscribe to to another ASM Journal go to: **http://journals.asm.org/site/subscriptions/**

Journals.ASM.org

Downloaded from http://jvi.asm.org/ on September 25, 2013 by UNIV OF TENNESSEE

JVI Journals.ASM.org

Frog Virus 3 Open Reading Frame 97R Localizes to the Endoplasmic Reticulum and Induces Nuclear Invaginations

Brooke A. Ring,* Andressa Ferreira Lacerda, Dylan J. Drummond, Christina Wangen, Heather E. Eaton,* Craig R. Brunetti

Department of Biology, Trent University, Peterborough, Ontario, Canada

Frog virus 3 (FV3) is the type species of the genus *Ranavirus*, family *Iridoviridae*. The genome of FV3 is 105,903 bases in length and encodes 97 open reading frames (ORFs). The FV3 ORF 97R contains a B-cell lymphoma 2 (Bcl-2) homology 1 (BH1) domain and has sequence similarity to the myeloid cell leukemia-1 (Mcl-1) protein, suggesting a potential role in apoptosis. To begin to understand the role of 97R, we characterized 97R through immunofluorescence and mutagenesis. Here we demonstrated that 97R localized to the endoplasmic reticulum (ER) at 24 h posttransfection. However, at 35 h posttransfection, 97R localized to the ER but also began to form concentrated pockets continuous with the nuclear membrane. After 48 h posttransfection, 97R was still localized to the ER, but we began to observe the ER and the outer nuclear membrane invaginating into the nucleus. To further explore 97R targeting to the ER, we created a series of C-terminal transmembrane domain deletion mutants. We found that deletion of 29 amino acids from the C terminus of 97R abolished localization to the ER. In contrast, deletion of 12 amino acids from the C terminus of 97R did not affect 97R localization to the ER. In addition, a hybrid protein containing the 97R C-terminal 33 amino acids was similarly targeted to the ER. These data indicate that the C-terminal 33 amino acids of 97R are necessary and sufficient for ER targeting.

Iridoviridae family members are large (120 to 200 nm), double-stranded DNA (dsDNA) viruses that are both circularly permutated and terminally redundant. The genomic size of members of the family *Iridoviridae* ranges from 105,903 to 212,482 bases in length. The *Iridoviridae* family consists of five genera, *Iridovirus*, *Chloroiridovirus*, *Megalocytivirus*, *Lymphocystivirus*, and *Ranavirus*. Frog virus 3 (FV3) is the type species for the *Ranavirus* genus, was originally isolated from a renal tumor of a leopard frog (*Rana pipiens*), and was later discovered to primarily infect the kidneys of tadpoles and adult frogs (1, 2). FV3 is found worldwide and has been reported to cause mortality rates as high as 90% in American bullfrog populations (3, 4).

FV3, like all other iridoviruses, contains a set of 26 conserved genes involved in essential viral functions, such as DNA replication and transcriptional regulation (5). The FV3 genome also contains a variety of genes involved in virus-host interactions. Specifically, FV3 contains several genes that may act to manipulate the host immune response in order to enhance replication in the host. For example, open reading frame (ORF) 64R contains both a caspase recruitment domain (CARD) and a DEATH domain-like motif, and ORF 97R, which has similarity to a B-cell lymphoma 2 (Bcl-2)-like protein, putatively plays roles in apoptosis (2).

Apoptosis is a complex biochemical process that results in the death of a cell. Many viruses inhibit, delay, or promote apoptosis (6). Viruses in the *Iridoviridae*, including FV3, cause apoptosis upon infection (7–11). FV3-infected fathead minnow (FHM) cells showed signs of DNA fragmentation at 6 to 7 h postinfection (7). It was further shown that the use of caspase inhibitors blocked FV3-induced apoptosis, indicating that the apoptotic trigger involves a caspase cascade (7). The induction of apoptosis following FV3 infection was suggested to be the result of a block in cellular translation (7).

Apoptosis is generally mediated by mitochondrial regulation of the Bcl-2 family of proteins, which direct both the induction and inhibition of apoptosis and operate between the mitochondrion and the endoplasmic reticulum (ER) (12–14). Each member of the Bcl-2 family contains a Bcl-2 homology (BH) domain, and there are four BH domains in total, BH1, BH2, BH3, and BH4. Bcl-2 family members containing all BH domains (BH1 to BH4) are antiapoptotic, while proteins with domains BH1 to BH3 are proapoptotic (15). Many Bcl-2 family members contain only a BH3 domain (13). Almost all of the Bcl-2 family members also contain a tail anchor, which is a C-terminal transmembrane domain that mediates specific membrane targeting (13). The BH domains and transmembrane domains are used as binding sites for homo- and heterodimerization with other Bcl-2 proteins (6, 15, 16).

Each of the BH domains can act independently as binding sites for the Bcl-2 family. The BH1 and BH2 domains are the best-conserved domains and are known as death repressor domains. The BH1 and BH2 domains are pivotal in the antiapoptotic abilities of the Bcl-2 and Bcl-XL proteins (17). Bcl family members that possess only a BH3 domain are proapoptotic and act in either extrinsic or intrinsic pathways (13). The BH3 domain is a death-promoting domain, consisting of a 16-amino-acid alpha helix (14, 15). The BH3 domain is a key regulator of the homo- and heterodimerization interactions between all Bcl-2 family members (18). The BH4 domain is found only in antiapoptotic Bcl-2 proteins and thus mainly functions as a death repressor domain (19,

Received 5 March 2013 Accepted 8 June 2013

Published ahead of print 12 June 2013

Address correspondence to Craig R. Brunetti, craigbrunetti@trentu.ca.

* Present address: Brooke A. Ring, Department of Pathology and Molecular Medicine, Queen's University, Kingston, Ontario, Canada; Heather E. Eaton, Department of Medical Microbiology and Immunology, University of Alberta, Edmonton, Alberta, Canada.

B.A.R. and A.F.L. contributed equally to this article.

Copyright © 2013, American Society for Microbiology. All Rights Reserved.

doi:10.1128/JVI.00637-13

20). Deletion of the BH4 domain in antiapoptotic Bcl-2 proteins resulted in the loss of their ability to inhibit apoptosis, but these mutants were still able to form homo- and heterodimers. It has recently been established that the stress response of the ER may also play a role in apoptosis (21). The ER stress response may be the result of heat or radiation exposure or fluctuating Ca^{2+} levels or, more likely, is caused by a rapid influx of unfolded, misfolded, or mutated proteins (14, 21, 22). If the ER cannot correct the problem of an influx of unfolded, misfolded, or mutated proteins, the unfolded protein response (UPR) is triggered (21). The UPR primarily restores the homeostasis of the ER, but if this is not possible, apoptosis is triggered (23, 24). The UPR is triggered when Bcl-2 family members Bak and Bax activate IRE1, a protein that mediates the activation of membrane-bound GRP78 (17). The activation of GRP78 ultimately leads to the upregulation of production of CCAAT-enhanced-binding protein (CHOP), which downregulates Bcl-2 proteins in the mitochondria (25). The downregulation of Bcl-2 causes the release of cytochrome *c*, which eventually leads to apoptosis (26, 27).

The Bcl-2 family of proteins also functions in other aspects of the ER stress response (15). For example, the Bcl-2 family maintains ER homeostasis through regulation of Ca^{2+} levels. Bcl-2 and Bcl-XL are key modulators of Ca^{2+} channels of the ER (14). Bcl-2 and Bcl-XL prevent the release of Ca^{2+} from the ER by binding to the inositol 1,4,5-trisphosphate receptor (IP_3R) Ca^{2+} channel via their BH4 domains (14, 28). However, when ER stress is triggered, BH3-containing Bcl-2 family members, which either reside in the ER (Bik) or translocate to the ER from the cytoplasm (Bim and Bax), inhibit the activity of Bcl-2 and Bcl-XL to regulate Ca^{2+} channels (17). This results in the release of Ca^{2+} into the cytoplasm, causing a cascade leading to apoptosis (17, 26).

FV3 ORF 97R encodes a 137-amino-acid protein and contains 2 potential BH domains. ORF 97R displays early and late expression (29). It is not known if this is a technical anomaly or if it reflects the reactivation of gene expression at late times after infection or the use of alternate promoters (29). ORF 97R was reported to share 36% sequence similarity with myeloid cell leukemia-1 (Mcl-1) protein (2). The sequence similarity between 97R and Mcl-1 is most highly conserved within the BH1 domain. Additionally, the 97R C terminus contains hydrophobic amino acids, characteristic of a C-terminal transmembrane domain, which many Bcl-2 family members possess. It is possible that 97R may interact with apoptotic machinery, due to its sequence similarity to Mcl-1, its BH1 domain, and its potential C-terminal transmembrane domain. In order to begin to characterize 97R, its expression and how it changes over time were investigated. Furthermore, 97R deletion and truncation mutants with mutations in the BH1 domain and C-terminal transmembrane domain were examined to determine their role in 97R localization.

MATERIALS AND METHODS

Cell lines and reagents. The baby green monkey kidney (BGMK), human embryonic kidney 293T (HEK293T), bluegill fry 2 (BF2), and FHM cell lines were obtained from the American Type Culture Collection (ATCC; Manassas, VA). Both BGMK and HEK293T cells were cultured with Dulbecco's modified Eagle's medium (DMEM; Thermo Scientific, Logan, UT) with 7% fetal bovine serum (FBS; Thermo Scientific, Logan, UT) (BGMK cells) or 10% FBS (HEK 293T cells), 2 mM L-glutamine, and 100 U/ml penicillin and were maintained at 37°C with 5% CO_2. BF2 cells were cultured with Eagle's minimum essential medium (EMEM; Thermo Scientific) with Earle's balanced salts including 10% FBS, 2 mM L-glutamine, 100 U/ml penicillin, 5 mM nonessential amino acids, 5 mM sodium pyruvate, and 5 mM amphotericin B and were maintained at 26°C with 5% CO_2. FHM cells were cultured in EMEM with 10% FBS, 100 U/ml penicillin, 100 U/ml streptomycin, and 10% amphotericin B, and cells were maintained at 30°C. All cells were maintained in closed culture flasks (Sarstedt, Montreal, QC, Canada).

Isolation of viral DNA. FHM cells were grown to 80% confluence and were infected with FV3 VR-567 (ATCC) at a multiplicity of infection (MOI) of 0.1. The infection was allowed to progress until cytopathic effects (CPEs) were observed. Cells were then harvested, resuspended in 1 ml phosphate-buffered saline (PBS), and freeze-thawed three times at −80°C. An equal volume of phenol-chloroform was added, and the aqueous phase was transferred to a fresh tube containing 10% (vol/vol) 5 M sodium acetate and 200% (vol/vol) ethanol (96%). The mixture was left for 15 min on ice, followed by centrifugation at 10,000 × *g* for 10 min; the pellet was then air dried and resuspended in PBS.

Codon optimization. ORF 97R was codon optimized by GenScript (Piscataway, NJ) and cloned into plasmid pDREAM2.1 with an N-terminal FLAG tag (GenScript).

PCR. PCR mixtures contained 100 ng of viral DNA, 10 μM forward and reverse primers, 1× PCR buffer (Invitrogen, Burlington, ON, Canada), 2.5 mM $MgCl_2$ (Invitrogen), 2.5 mM deoxynucleoside triphosphates (Sigma-Aldrich, Oakville, ON, Canada), and 2.5 U *Taq* DNA polymerase (5 U/μl; Invitrogen). The reaction was cycled using the cycling conditions 94°C for 30 s, 52°C for 1 min, and 72°C for 1 min 30 s for 30 cycles.

Cloning. PCR products were cloned using a pTARGET mammalian expression vector system (Promega, Madison, WI). In a 0.6-ml tube, 3 μl of double-distilled H_2O (ddH_2O), 1 μl 10× T4 DNA ligase buffer, 4 μl (4 ng/μl) PCR product, 1 μl (60 ng/μl) pTARGET vector, and 1 μl T4 DNA ligase were mixed and placed at 4°C overnight.

Vector construction for 64-97R and 97R BH mutant proteins. Mutant proteins 64-97R and 97R BH (97R BH mut) were synthesized by GenScript. A myc tag was added to 64-97R using 10 ng of DNA and the following primers: 5′-ATGGAACAGAAACTGATTAGCG-3′ (64-97R forward), 5′-TCAGTAGAACAGCAGAGACAG-3′ (64-97R and 97R BH mut reverse), and 5′-ATGCTGGTTTTTGATTAAACGCCT-3′ (97R BH mut forward). The PCR product was cloned using the pTARGET mammalian expression vector system (Promega) as per the manufacturer's protocol.

TUNEL assay. A Click-it terminal deoxynucleotidyltransferase-mediated dUTP-biotin nick end labeling (TUNEL) Alexa Fluor 488 kit (Invitrogen) was used to detect DNA fragmentation in samples that were transfected with 97R. The cells were fixed, stained, and analyzed using a confocal microscope.

Transformation. In a 15-ml culture tube, 2 μl of the ligated pTarget reaction mixture was mixed with 75 μl of *Escherichia coli* DH5α (Invitrogen) and placed on ice for 1 h, and samples were heat shocked for 1 min at 42°C and placed on ice for 2 min. Five hundred microliters of LB broth (10 g tryptone, 10 g NaCl, 5 g yeast extract, 1 liter ddH_2O) was added, and the mixture was then incubated at 37°C for 1 h. Two hundred fifty microliters of the transformation mixture was plated on plates containing ampicillin (20 μg/ml) with blue/white selection (4 μl of 0.1 M IPTG [isopropyl-β-D-thiogalactopyranoside] and 40 μl of 20 mM X-Gal [5-bromo-4-chloro-3-indolyl-β-D-galactopyranoside]) and left to incubate for 18 to 24 h.

Midiprep. Bacterial colonies were grown in 3 ml LB broth and 100 μg/ml of ampicillin (Sigma-Aldrich, Oakville, ON, Canada) with shaking at 250 rpm and 37°C for 6 h. Three-milliliter cultures were transferred to larger flasks containing 50 ml LB broth with 100 μg/ml of ampicillin and shaken at 250 rpm at 37°C overnight. Midipreps were performed as described by Sambrook and Russell (30). Five microliters of sample was mixed with 5 μl of ddH_2O, 2 μl loading dye and loaded on a 1% agarose gel. DNA bands were visualized on a UV illuminator.

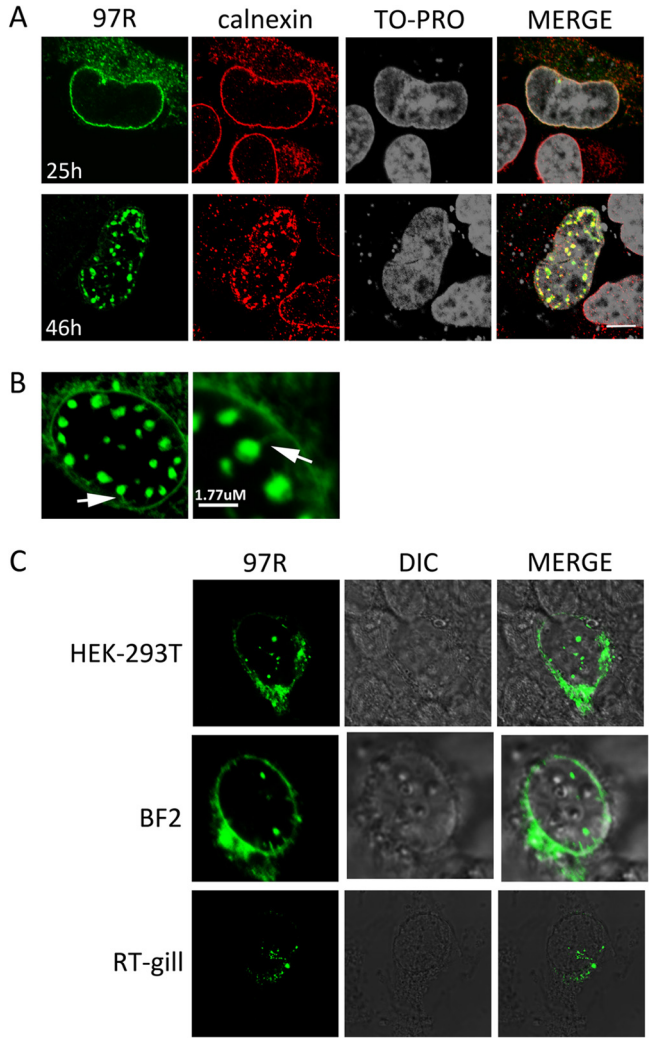

FIG 1 97R localizes to the ER. (A) BGMK cells were transiently transfected with 97R. At 25 and 46 h posttransfection, indirect immunofluorescence was performed to detect 97R (anti-FLAG; green), the ER membrane (anticalnexin; red), and the nucleus (TO-PRO; gray). (B) Higher-magnification view of BGMK cells transiently transfected with 97R. At 46 h posttransfection, indirect immunofluorescence was performed to detect 97R (anti-FLAG; green)-induced invagination structures. White arrows, invagination stalk. (C) HEK293T, BF2, and RT-gill cells were transiently transfected with 97R. At 46 h posttransfection, indirect immunofluorescence was performed to detect 97R (anti-FLAG; green). Differential interference contrast (DIC) was used to visualize the cells' nuclei, and images were captured using a laser scanning confocal microscope.

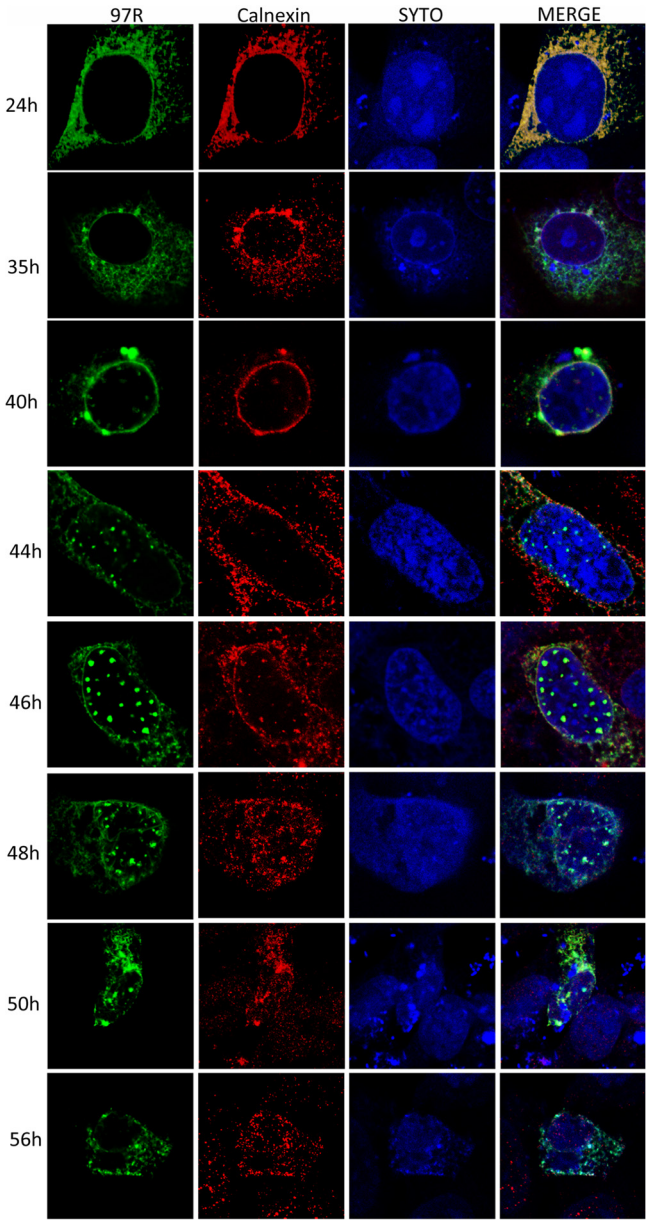

FIG 2 Kinetics of 97R expression. BGMK cells were transiently transfected with 97R, and at 24, 35, 40, 44, 46, 48, 50, or 56 h posttransfection indirect immunofluorescence was performed to detect 97R (anti-FLAG; green), the ER membrane (anti-calnexin; red), and the nucleus (SYTO 17; blue). Images were captured on a laser scanning confocal microscope.

Transfection. BGMK, HEK293T, RT-gill, and BF2 cells were grown to 60 to 70% confluence in 6-well plates with coverslips. In a sterile, 1.5-ml centrifuge tube, 200 μl of serum-free DMEM (Thermo Scientific), 20 μl of 50 mg/μl polyethylenimine (PEI; Fisher Scientific, Ottawa, ON, Canada), and 4 μl of 10 μg/μl plasmid DNA were mixed and left to incubate at room temperature for 15 min. Transfection complexes were then added to the cells with 1 ml fresh medium.

Immunofluorescence. Cells in 6-well plates with coverslips were washed twice with fresh PBS for 2-min intervals. PBS was removed and replaced with 1 ml 3.7% paraformaldehyde (0.444 g paraformaldehyde, 12 ml PBS, 3 μl 10 N NaOH) for 10 min. Cells were washed with PBS twice for 2-min intervals. The PBS was removed and replaced with 1 ml of 0.1 M Triton X-100 for 5 min. Cells were washed with fresh PBS twice for 2-min intervals, and the PBS was replaced with 2 ml block buffer (5% bovine serum albumin [BSA], 50 mM Tris-HCl [pH 7.4], 150 mM NaCl, 0.5% NP-40) for 1.5 h at room temperature. Cells were washed three times with fresh wash buffer (1% BSA, 50 mM Tris-HCl [pH 7.4], 150 mM NaCl, 0.5% NP-40) for 3-min intervals. The wash buffer was removed. Then, 100 μl of 1 mg/ml anti-FLAG M2 mouse primary antibody (diluted 1/500 in wash buffer; Sigma-Aldrich, Oakville, ON, Canada) was added to detect the FLAG tag in 97R and/or 200 μg/ml anti-protein disulfide isomerase (anti-PDI; an ER lumen marker) H-160 rabbit antibody (diluted 1/100 in wash buffer; Santa Cruz, Santa Cruz, CA), 200 μg/ml anti-Syne-1 (outer nuclear membrane marker) H-100 rabbit antibody (diluted 1/100 in wash buffer; Santa Cruz), 200 μg/ml anti-Nopp140 (nucleolus protein marker) H-80 rabbit antibody (diluted 1/100 in wash buffer; Santa Cruz), or 200

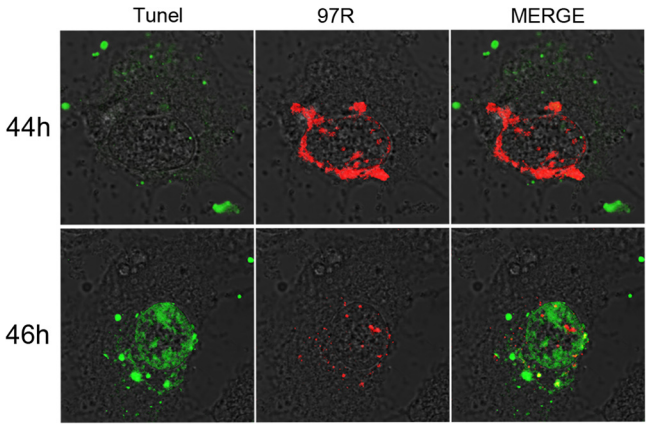

FIG 3 Cells transfected with 97R undergo apoptosis. BGMK cells were transfected with 97R, and at 44 and 46 h posttransfection the cells were fixed and stained for 97R (anti-FLAG, red) and a TUNEL assay was performed. Differential interference contrast (DIC) was used to visualize the cells' nuclei, and images were captured using a laser scanning confocal microscope.

μg/ml anticalnexin (ER integral marker) H-70 rabbit antibody (diluted 1/50 in wash buffer; Santa Cruz) was added to each coverslip for 1 h at room temperature. The antibody solution was removed, and cells were washed three times with fresh wash buffer for 3-min intervals. The wash buffer was removed, and 100 μl of secondary antibody, fluorescein isothiocyanate-conjugated goat anti-mouse immunoglobulin G (diluted 1/100 in wash buffer; Santa Cruz) and/or Cy3-conjugated goat anti-rabbit immunoglobulin G (diluted 1/200 in wash buffer; Santa Cruz), was added to each coverslip for 30 min at room temperature. The antibody solutions were removed, and cells were washed three times with fresh wash buffer for 3-min intervals. The wash buffer was removed, and 100 μl of nuclear and nucleolar stains, 1 mM TO-PRO-3 iodide (diluted 1/2,000 in wash buffer; Invitrogen) and/or SYTO 17 (diluted 1/5,000 in wash buffer; Invitrogen), was added directly to the coverslips and left for 15 min at room temperature. The antibody solution was removed and replaced with 1 ml PBS for 5 min. PBS was removed, and the cells were washed with fresh PBS twice for 2-min intervals. Coverslips were removed from the plate, mounted onto slides with Vectashield mounting medium with DAPI (4′,6-diamidino-2-phenylindole; Vector Laboratories, Burlington, ON, Canada), and sealed with clear nail polish. Immunofluorescence was detected using a Leica DM IRE2 fluorescence microscope (Leica, Concord, ON, Canada). Images were assembled using Adobe Photoshop CS4 software.

RESULTS

97R localizes to the ER and modifies the ER membrane. To begin the characterization, ORF 97R was codon optimized to induce adequate expression in primate cell lines. We transfected a plasmid expressing 97R into BGMK cells to determine the site of intracellular accumulation. At 25 h posttransfection, indirect immunofluorescence was performed and 97R was found to colocalize with the ER marker calnexin (Fig. 1A). Interestingly, at 25 h posttransfection, 97R was present in the ER; however, at 46 h, expression of 97R was observed in intranuclear structures (Fig. 1A), which were connected by a thin stalk to the ER/nuclear membrane (Fig. 1B). These intranuclear structures also stained positive for calnexin (Fig. 1A), suggesting that they were continuous with the ER and nuclear membrane. These data suggest that 97R initially localizes to the ER and over time induces invagination of the ER membrane into the nucleus.

To confirm that the expression of 97R to the ER and the induced invaginations were not cell type specific, 97R was transiently transfected into HEK293T (human), RT-gill (fish), and BF2 (fish) cell lines. At 46 h posttransfection, 97R expression altered the ER membrane and caused nuclear invaginations in all three cell lines (Fig. 1C). These data suggest that 97R induces the invagination of the nuclear membrane in a variety of cell

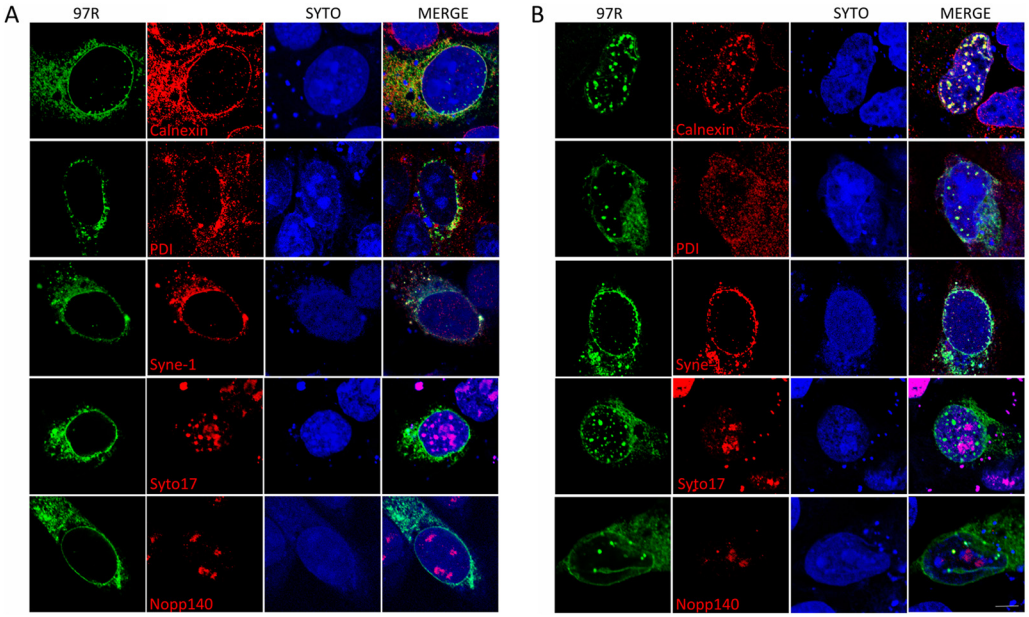

FIG 4 97R-induced invaginations contain the ER and the outer nuclear membrane. BGMK cells were transiently transfected with 97R for 24 h (A) or 48 h (B). Indirect immunofluorescence was used to detect expression of 97R (anti-FLAG; green), the ER membrane (anticalnexin), ER lumen (anti-PDI), nucleolar chaperone protein (anti-Nopp140), outer nuclear membrane (anti-Syne-1), nucleoli (SYTO 17), and nucleus (TO-PRO; blue). Images were captured using a laser scanning confocal microscope.

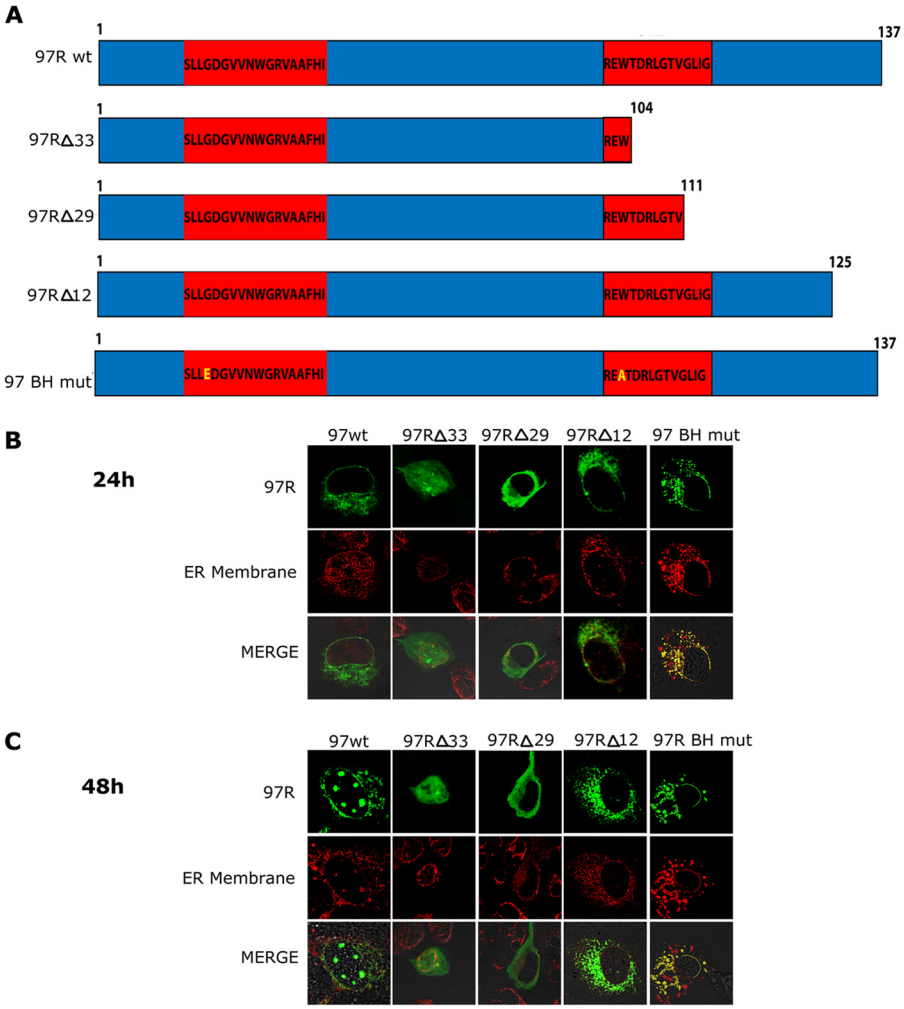

FIG 5 Deletion of the C terminus of 97R alters its localization. (A) Schematic of wild-type (137 amino acids) and mutant forms of 97R. Red boxes, potential BH domains. BGMK cells were transiently transfected with wild-type 97R (97Rwt) or one of the 97R mutants (97RΔ33, 97RΔ29, 97RΔ12, or 97RBH mut). At 24 h (B) and 48 h (C) posttransfection, indirect immunofluorescence was performed to detect 97R (anti-FLAG; green), and either the ER membrane (anticalnexin; red for 97Rwt, 97RΔ33, 97RΔ12, and 97R BH mut) or the ER lumen (anti-PDI; red for 97RΔ29) was detected. Images were captured on a laser scanning confocal microscope.

lines, including fish cell lines, a natural host of FV3, but it appears that the extent of invaginations differs according to cell type.

97R expression alters the ER membrane over time and is related to apoptosis. To determine the kinetics of the formation of the 97R-induced invaginations, we transfected 97R into BGMK cells and at 24, 35, 40, 44, 46, 48, 50, and 56 h posttransfection we examined 97R expression. At 24 h posttransfection, 97R localized to the ER (Fig. 2). At 35 and 40 h posttransfection, we began to observe 97R expression in the ER, as well as the development of pockets of 97R expression continuous with the nuclear membrane, which continued to stain positive for calnexin (Fig. 2). At between 44 and 48 h posttransfection 97R expression invaginated into the nucleus, at 50 h posttransfection the cell began to reduce in size (Fig. 2), and at 56 h posttransfection the levels of 97R expression appeared to decrease. 97R expression was rarely observed past 68 h posttransfection, and no 97R expression was detected by 72 h posttransfection (results not shown).

A TUNEL assay was performed to determine if the apparent deterioration of the cell at 50 h posttransfection and later was due to the induction of apoptosis by 97R. We transfected 97R into BGMK cells and examined the induction of apoptosis at a variety of time points posttransfection. At 44 h and earlier times posttransfection, we did not observe a positive signal from the TUNEL assay kit (Fig. 3; data not shown), suggesting that induction of apoptosis had not occurred. However, at time points beginning at 46 h and later, we observed positive TUNEL assay staining (Fig. 3; data not shown), suggesting that at later time points, apoptosis induction was occurring in the presence of 97R.

97R-induced invaginations colocalize with the ER and outer nuclear membrane. To gain a greater understanding of the membranes that are invaginating into the nucleus, we transfected 97R into BGMK cells and examined a variety of ER and nuclear membrane markers at 24 h (Fig. 4A) and 48 h (Fig. 4B) posttransfection. 97R colocalized with ER luminal PDI (16) and Syne-1, which localized to the outer nuclear membrane (Fig. 4) (28). In addition, 97R colocalized with the ER integral protein calnexin (Fig. 4).

These data suggest that both luminal and integral proteins of the ER, as well as the outer nuclear membrane, appear to invaginate into the nucleoplasm.

To determine whether these invaginations interacted with the nucleolus, two nucleolar markers, Nopp140 and SYTO 17, were used at 24 and 48 h posttransfection (Fig. 4). We did not observe any colocalization between the 97R-induced invaginations and the nucleolus. This suggests that 97R-induced invaginations are not interacting with the nucleolus (Fig. 4).

The C terminus of 97R is responsible for the ER localization. To determine whether localization of 97R to the ER was the result of a potential C-terminal transmembrane domain, a series of C-terminal deletion mutants was created. A transmembrane domain usually comprises highly hydrophobic amino acid stretches (31). According to the hydrophobic content, the longest potential transmembrane domain in 97R is between residues 104 and 137 (97RΔ33) (Fig. 5A), while the shortest potential transmembrane domain is between residues 125 and 137 (97RΔ12) (Fig. 5A). Three deletion mutants were constructed and transfected into BGMK cells, and at 24 h posttransfection, 97RΔ33 was found to localize to the cytoplasm and nucleoplasm, while 97RΔ29 localized to the cytoplasm alone (Fig. 5B and C). In contrast, 97RΔ12 localized to the ER, but no invaginations of the ER were observed even at 48 h posttransfection (Fig. 5B and C). These data suggest that 97R's highly hydrophobic C-terminal transmembrane domain composed of 29 amino acids is required for localization of 97R to the ER and the C-terminal 12 amino acids are necessary for nuclear invaginations.

Since BH domains mediate binding to other proteins, we wanted to explore whether the BH domains of 97R were also responsible for targeting to the ER. The mutations on the BH domain of 97R were designed on the basis of the data obtained from Clohessy et al. (32). They found that mutations at the Mcl-1 BH1 (G55E) and BH2 (W104A) domains resulted in failure to interact with the glutathione *S*-transferase–tBid death receptor. Since 97R has similarity to the BH domains of Mcl-1, we mutated the BH domains of 97R to contain the corresponding Mcl-1-inactivating mutations (97R BH mut) (Fig. 5A) and transfected the construct into BGMK cells. 97R BH mut localized to the ER membrane; however, no nuclear invaginations were observed at either the 24- or 48-h-posttransfection time point of expression (Fig. 5B and C). Although the BH domains of 97R are not responsible for the localization to the ER, they may be required for the formation of the nuclear invaginations.

The C terminus of 97R is necessary and sufficient for ER targeting and nuclear invagination. To investigate whether the C terminus of 97R was sufficient for ER localization, the 33-amino-acid sequence from the C terminus of 97R was inserted at the C terminus of the FV3 gene 64R (Fig. 6A), which normally localizes to the cytoplasm (Fig. 6B). This hybrid protein was named 64-97R (Fig. 6A). At 24 to 42 h posttransfection, 64-97R exhibited typical ER localization (Fig. 6C). However, at 46 h we began to observe the formation of nuclear invaginations (Fig. 6C). Finally, at 50 h postinfection the cells displayed a cytopathic effect similar to that seen in cells transfected with a full-length 97R expression vector (Fig. 6C). These data support the role of 97R's hydrophobic C-terminal transmembrane domain in localization to the ER and in the formation of nuclear invaginations.

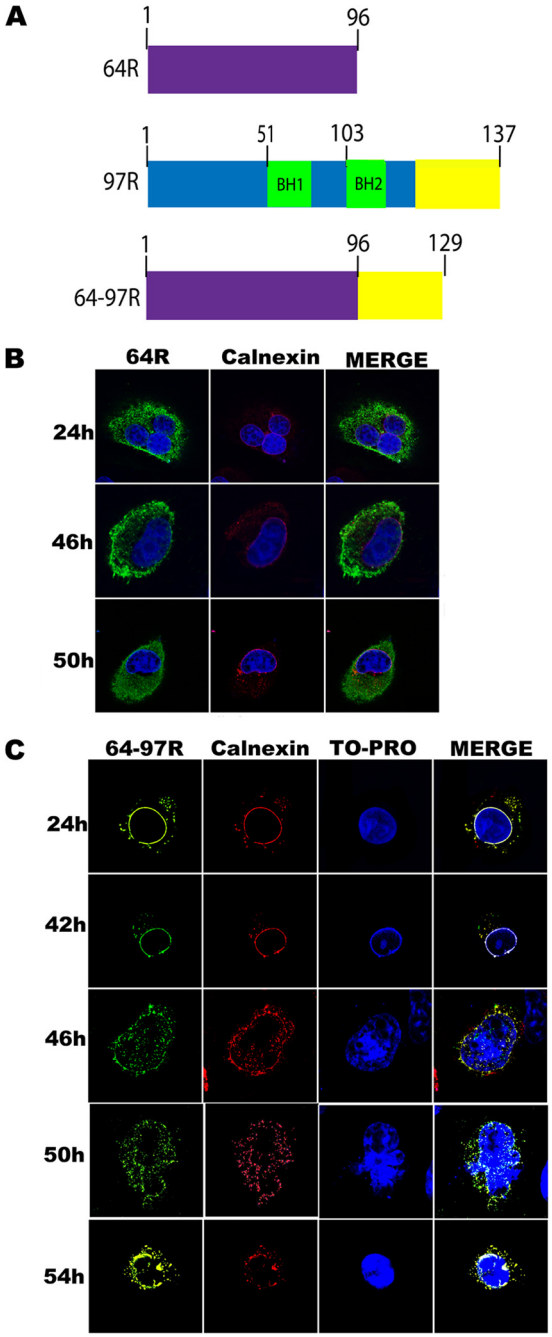

FIG 6 The 97R C-terminal tail alters localization of 64R and induces ER invaginations. (A) Schematic of wild-type 64R (purple) along with wild-type 97R. The BH domains of 97R are highlighted in green, while the C-terminal 33 amino acids of 97R are highlighted in yellow. The 64-97R fusion protein contains the entire wild-type 64R fused to the C-terminal 33 amino acids (yellow) of 97R. (B) BGMK cells were transfected with myc-64R, and after 24, 46, or 50 h the cells were fixed and stained for 64R (anti-myc; green) and calnexin (red). Nuclei were stained with TO-PRO (blue), and images were captured on a laser scanning confocal microscope. (C) BGMK cells were transiently transfected with myc-tagged 64-97R, and at 24, 42, 46, 50, or 54 h posttransfection the cells were fixed and indirect immunofluorescence was performed to detect 64-97R (anti-myc; green), the ER membrane (anticalnexin; red), and the nucleus (TO-PRO; blue). Images were captured on a laser scanning confocal microscope.

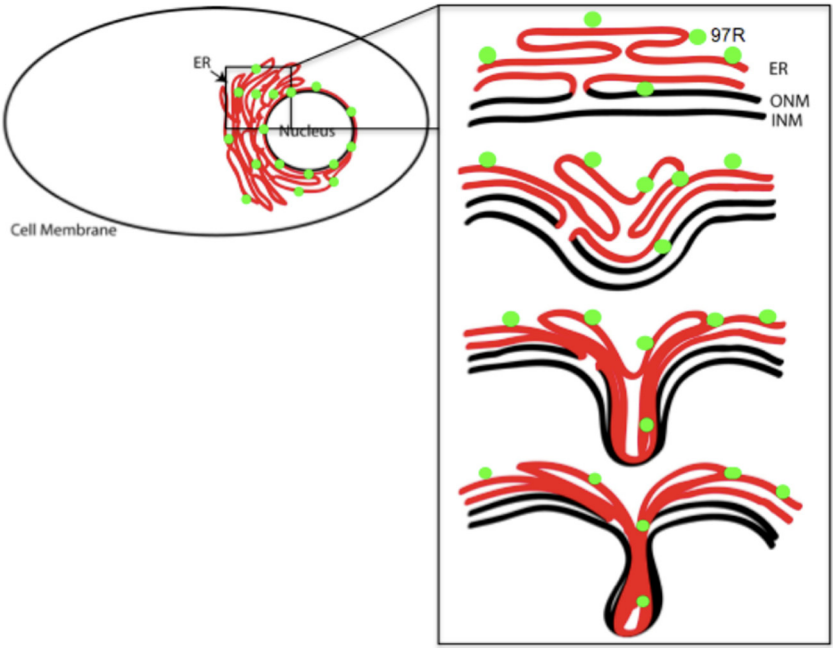

FIG 7 Model of 97R-induced invagination of the ER and outer nuclear membrane into the nucleus. The proposed model of 97R invaginations is composed of the ER membrane (red), the outer nuclear membrane (ONM), and the inner nuclear membranes (INM; black). Green circles, the 97R protein.

DISCUSSION

Our results demonstrate that FV3 ORF 97R localizes to the ER membrane, where it alters the membrane conformation over time (Fig. 1 to 3). 97R expression causes the invagination of the ER and outer nuclear membrane into the nucleus (Fig. 4). Additionally, it was determined that the C terminus of 97R is necessary and sufficient for localization to the ER membrane and induction of nuclear invaginations.

Nuclear invaginations have previously been reported. The nuclear envelope can contain convolutions, including a deep, branching invagination named the nucleoplasmic reticulum (NR), which has been reported in a variety of normal and abnormal cells; moreover, the nucleoplasmic reticulum is abundant in many tumor cell types (33, 34). The nucleoplasmic reticulum is neither restricted to a specific cell or tissue nor dependent on a specific developmental stage (35). Furthermore, the nucleoplasmic reticulum morphology is altered in some pathologies, suggesting that their regulatory mechanisms are susceptible to pathological dysregulation (8, 34). In addition, nuclear invaginations were induced through the overexpression of transfected nucleolar chaperone protein Nopp140 (R rings) (36) as well as a truncated mutant of fibroblast growth factor receptor 4 (FGFR4), in which removal of 300 amino acids from its intracellular portion and 285 amino acids from its extracellular portion was also able to alter the nuclear membrane (37). Nuclear invaginations caused by these proteins were found to contain ER and the inner nuclear membrane, but there was no evidence of outer nuclear membrane complexes (37, 38). These studies proposed that the structures were the result of the invagination of the ER and the inner nuclear membrane but not the outer nuclear membrane (36, 37). The nuclear invaginations were postulated to derive from Nopp140 and truncated FGFR4 amino acid residues interacting with the ER and inner nuclear membrane. It was established that Nopp140 and truncated FGFR4 contained rich clusters of arginine and serine residues, which were found to be required for the formation of nuclear invaginations (36, 37). Additionally, it was also found that the serine residues on both Nopp140 and truncated FGFR4 required phosphorylation to form the nuclear invaginations (37).

In contrast, invaginations of 97R possess outer nuclear membrane proteins, as observed by colocalization with Syne-1. In addition, 97R lacks clusters of serine or arginine residues, which have been shown in other studies to be essential for the formation of nuclear invaginations. We speculate that 97R causes the ER and the outer and inner nuclear membranes to invaginate into the nucleoplasm (Fig. 7) as a result of 97R interacting with itself or another unknown protein. However, we have shown that the C-terminal 33 amino acids of 97R are necessary and sufficient for the formation of the nuclear invaginations.

To determine if the localization of 97R to the ER was a result of its potential C-terminal transmembrane domain, several deletion mutants were created. It was determined that 29 residues of the C terminus are required for 97R localization to the ER, suggesting that it is possible that 97R's transmembrane domain is a tail anchor. It was also demonstrated that the addition of 33 residues of the C terminus of 97R to 64R could change the localization of 64R from the cytoplasm to the ER. These data together provide evidence that the C terminus of 97R is necessary and sufficient for ER targeting and nuclear invaginations. Proteins with short, hydrophobic tail anchors may be retained specifically to the ER, while proteins with longer, hydrophilic tail anchors may travel to the mitochondria (24, 39). Tail anchors do not contain upstream signaling sequences, allowing the N terminus of proteins to remain exposed to the cytosol and the C terminus of proteins to remain anchored to a membrane (24, 39).

To determine if the BH1 domain was also responsible for targeting 97R to the ER, a deletion mutant was created. 97R's BH1 deletion mutant localized to the ER, suggesting that the BH1 domain is not responsible for 97R's localization to the ER. We speculate that the BH1 domain may be responsible for the formation of 97R's invaginations by acting as a binding site for protein-protein interactions.

In this study, we have determined that 97R localizes to the ER. Over time, 97R expression alters the ER membrane by inducing invaginations of the ER and the outer nuclear membrane into the nucleoplasm. Nuclear invaginations are a relatively rare phenomenon, and the 97R-induced invaginations are distinct from the invaginations previously characterized in other systems. Although this study did not explore the role of 97R in a viral infection, future work will define the role that 97R plays in a viral infection. Understanding the role of nuclear invaginations in an FV3 infection will be complicated by the fact that FV3 induces apoptosis, including DNA fragmentation (7) as well as fragmentation of the nucleus late in infection (data not shown). Thus, there are significant alterations happening to the nucleus in an FV3 infection, and it will be challenging to differentiate those events triggered by apoptotic responses versus those induced by 97R.

It is important to note that the nuclear invagination induced by 97R may point to unique viral perturbation happening in the cell. It is possible that other viral proteins in other systems may induce similar morphological changes in the cell. Future studies could further characterize the formation of the nuclear invaginations (Fig. 7) and investigate possible 97R homo- or heterotypic interactions, which may be critical in understanding 97R's function in an FV3 infection.

ACKNOWLEDGMENTS

This work is supported by Discovery Grants (Natural Science and Engineering Research Council [NSERC] of Canada) to C.R.B. H.E.E. is the recipient of an NSERC postgraduate scholarship, and D.J.D. is the recipient of an NSERC undergraduate research award.

REFERENCES

1. **Granoff A, Came PE, Breeze DC.** 1966. Viruses and renal carcinoma of Rana pipiens. 1. The isolation and properties of virus from normal and tumor tissue. Virology **29:**133–148.
2. **Tan WGH, Barkman TJ, Chinchar VG, Essani K.** 2004. Comparative genomic analyses of frog virus 3, type species of the genus Ranavirus (family Iridoviridae). Virology **323:**70–84.
3. **Daszak P, Berger L, Cunningham AA, Hyatt AD, Green DE Speare R.** 1999. Emerging infectious diseases and amphibian population declines. Emerg. Infect. Dis. **5:**735–748.
4. **Miller DL, Rajeev S, Gray MJ, Baldwin CA.** 2007. Frog virus 3 infection, cultured American bullfrogs. Emerg. Infect. Dis. **13:**342–343.
5. **Eaton H, Metcalf J, Penny E, Tcherepanov V, Upton C, Brunetti C.** 2007. Comparative genomic analysis of the family Iridoviridae: reannotating and defining the core set of iridovirus genes. Virol. J. **4:**11–27.
6. **Cuconati A, White E.** 2002. Viral homologs of BCL-2: role of apoptosis in the regulation of virus infection. Genes Dev. **16:**2465–2478.
7. **Chinchar VG, Bryan L, Wang J, Long S, Chinchar GD.** 2003. Induction of apoptosis in frog virus 3-infected cells. Virology **306:**303–312.
8. **Echevarria W, Leite MF, Guerra MT, Zipfel WR, Nathanson MH.** 2003. Regulation of calcium signals in the nucleus by a nucleoplasmic reticulum. Nat. Cell Biol. **5:**440–446.
9. **Imajoh M, Sugiura H, Oshima S.** 2004. Morphological changes contribute to apoptotic cell death and are affected by caspase-3 and caspase-6 inhibitors during red sea bream iridovirus permissive replication. Virology **322:**220–230.
10. **Lin PW, Huang YJ, John J, Chang YN, Yuan CH, Chen WY, Yeh CH, Shen ST, Lin FP, Tsui WH, Chang CY.** 2008. Iridovirus Bcl-2 protein inhibits apoptosis in the early stage of viral infection. Apoptosis **13:**165–176.
11. **Paul ER, Chitnis NS, Henderson CW, Kaul RJ, D'Costa SM, Bilimoria SL.** 2007. Induction of apoptosis by iridovirus virion protein extract. Arch. Virol. **152:**1353–1364.
12. **Gewies A.** 2003. Introduction to apoptosis, p 26. *In* ApoReview. Max-Planck-Institute for Biochemistry, Martinsried, Germany.
13. **Wang CX, Youle RJ.** 2009. The role of mitochondria in apoptosis. Annu. Rev. Genet. **43:**95–118.
14. **Weston RT, Puthalakath H.** 2010. Endoplasmic reticulum stress and BCL-2 family members, p 65–77. *In* Hetz C (ed), BCL-2 protein family. Springer, New York, NY.
15. **Brunelle JK, Letai A.** 2009. Control of mitochondrial apoptosis by the Bcl-2 family. J. Cell Sci. **122:**437–441.
16. **Mayer B, Oberbauer R.** 2003. Mitochondrial regulation of apoptosis. News Physiol. Sci. **18:**89–94.
17. **Szegezdi E, MacDonald DC, Chonghaile TN, Gupta S, Samali A.** 2009. Bcl-2 family on guard at the ER. Am. J. Physiol. Cell Physiol. **296:**C941–C953.
18. **Lutz RJ.** 2000. Role of the BH3 (Bcl-2 homology 3) domain in the regulation of apoptosis and Bcl-2-related proteins. Biochem. Soc. Trans. **28:**51–56.
19. **Essbauer S, Bremont M, Ahne W.** 2001. Comparison of the eIF-2 alpha homologous proteins of seven ranaviruses (Iridoviridae). Virus Genes **23:**347–359.
20. **Huang Y, Huang X, Liu H, Gong J, Ouyang Z, Cui H, Cao J, Zhao Y, Wang X, Jiang Y, Qin Q.** 2009. Complete sequence determination of a novel reptile iridovirus isolated from soft-shelled turtle and evolutionary analysis of Iridoviridae. BMC Genomics **10:**224–238.
21. **Boyce M, Yuan J.** 2006. Cellular response to endoplasmic reticulum stress: a matter of life or death. Cell Death Differ. **13:**363–373.
22. **Schroder M, Kaufman RJ.** 2005. ER stress and the unfolded protein response. Mutat. Res. **569:**29–63.
23. **Rutkowski DT, Kaufman RJ.** 2004. A trip to the ER: coping with stress. Trends Cell Biol. **14:**20–28.
24. **Stewart TL, Wasilenko ST, Barry M.** 2005. Vaccinia virus F1L protein is a tail-anchored protein that functions at the mitochondria to inhibit apoptosis. J. Virol. **79:**1084–1098.
25. **Fawcett TW, Martindale JL, Guyton KZ, Hai T, Holbrook NJ.** 1999. Complexes containing activating transcription factor (ATF)/cAMP-responsive-element-binding protein (CREB) interact with the CCAAT enhancer-binding protein (C/EBP)-ATF composite site to regulate Gadd153 expression during the stress response. Biochem. J. **339:**135–141.
26. **Kumarswamy R, Chandna S.** 2009. Putative partners in Bax mediated cytochrome-c release: ANT, CypD, VDAC or none of them? Mitochondrion **9:**1–8.
27. **Wei MC, Lindsten T, Mootha VK, Weiler S, Gross A, Ashiya M, Thompson CB, Korsmeyer SJ.** 2000. tBID, a membrane-targeted death ligand, oligomerizes BAK to release cytochrome c. Genes Dev. **14:**2060–2071.
28. **Zhang QP, Skepper JN, Yang FT, Davies JD, Hegyi L, Roberts RG, Weissberg PL, Ellis JA, Shanahan CM.** 2001. Nesprins: a novel family of spectrin-repeat-containing proteins that localize to the nuclear membrane in multiple tissues. J. Cell Sci. **114**(Pt 24):4485–4498.
29. **Majji S, Thodima V, Sample R, Whitley D, Deng Y, Mao J, Chinchar VG.** 2009. Transcriptome analysis of frog virus 3, the type species of the genus Ranavirus, family Iridoviridae. Virology **391:**293–303.
30. **Sambrook J, Russell D.** 2001. Molecular cloning: a laboratory manual, 3rd ed. Cold Spring Harbor Laboratory Press, Cold Spring Harbor, NY.
31. **Borgese N, Colombo S, Pedrazzini E.** 2003. The tale of tail-anchored proteins. J. Cell Biol. **161:**1013–1019.
32. **Clohessy JG, Zhuang J, de Boer J, Gil-Gomez G, Brady HJM.** 2006. Mcl-1 interacts with truncated Bid and inhibits its induction of cytochrome c release and its role in receptor-mediated apoptosis. J. Biol. Chem. **281:**5750–5759.
33. **Clubb BH, Locke M.** 1998. 3T3 cells have nuclear invaginations containing F-actin. Tissue Cell **30:**684–691.
34. **Fischer AH, Taysavang P, Jhiang SM.** 2003. Nuclear envelope irregularity is induced by RET/PTC during interphase. Am. J. Pathol. **163:**1091–1100.
35. **Sarkar D, Emdad L, Lee SG, Yoo BK, Su ZZ, Fisher PB.** 2009. Astrocyte

elevated gene-1: far more than just a gene regulated in astrocytes. Cancer Res. **79:**8529–8535.
36. **Isaac C, Pollard JW, Meier UT.** 2001. Intranuclear endoplasmic reticulum induced by Nopp140 mimics the nucleolar channel system of human endometrium. J. Cell Sci. **114:**4253–4264.
37. **Sorensen V, Brech A, Khnykin D, Kolpakova E, Citores L, Olsnes S.** 2004. Deletion mutant of FGFR4 induces onion-like membrane structures in the nucleus. J. Cell Sci. **117:**1807–1819.
38. **Kittur N, Zapantis G, Aubuchon M, Santoro N, Bazett-Jones DP, Meier UT.** 2007. The nucleolar channel system of human endometrium is related to endoplasmic reticulum and R-rings. Mol. Biol. Cell **18:**2296–2304.
39. **Bulbarelli A, Sprocati T, Barberi M, Pedrazzini E, Borgese N.** 2002. Trafficking of tail-anchored proteins: transport from the endoplasmic reticulum to the plasma membrane and sorting between surface domains in polarised epithelial cells. J. Cell Sci. **115:**1689–1702.